

**IO'S UV-V ECLIPSE EMISSION: IMPLICATIONS FOR PELE-TYPE PLUMES.** C.H. Moore, D.B. Goldstein, P.L. Varghese, and L.M. Trafton, The University of Texas at Austin, (moorech@ices.utexas.edu).

**Introduction:** Io's atmospheric interaction with the Jovian plasma torus produces an intense UV-V aurora. Galileo images of Io in eclipse showed red, green, and blue glows from electron impact of both atomic and molecular species in Io's atmosphere. Two 12-minute exposures of Io's auroral spectrum from 1700–6000Å were taken with HST/STIS on August 7, 1999 during Io's eclipse [1]. We attempt to constrain the Pele-type volcanic activity by comparison of the observed and simulated spectra. Furthermore, the simulation spectra's sensitivity to inclusion of direct excitation of SO and the upstream electron temperature is examined.

**Model:** Io's eclipse MUV spectrum from ~2400 to 6000 Å is simulated with our Monte Carlo electron transport code previously applied to simulating Io's [OI] 6300 Å and [SII] 6716 Å aurora [2,3]. The code can compute both the electron and excited neutral dynamics. The electron guided center motion is simulated in pre-computed magnetic and electric fields [4]. During each timestep, the representative electrons move along the magnetic field lines and drift due to the electric field. After each move step the electrons collide probabilistically with the local neutral gas. Neutral gas dynamics and chemistry were included through the use of a pre-computed atmospheric model. The atmospheric model discussed in [3] is improved by having Pele-type plumes include an S<sub>2</sub> concentration of 15%. Also, the appropriate plumes for August, 1999 are active [7]. Figure 1 shows a schematic of the model. Finally, since the SO<sub>2</sub> MUV and S<sub>2</sub> emission is not forbidden, we assume the excited molecular state spontaneously decays at the electron-neutral interaction position.

**SO<sub>2</sub> MUV Spectrum:** In order to simulate Io's MUV spectrum, we use Ajello's [8] experimental cross section and spectral data for electron impact of SO<sub>2</sub> which produced SO band emission (MUV1) and SO<sub>2</sub> band emission (MUV2). The emitted photon wavelength is determined from an approximate spectrum generated by linear interpolation between two laboratory spectra at energies bracketing the electron energy. Since the threshold for MUV2 emission is 5.3eV and the lowest incident electron energy we have spectral data for is 8eV, we assume that the MUV2 emission spectrum does not change significantly for incident electrons below 8eV. For a given MUV excitation event the wavelength of the emitted photon is chosen via acceptance/rejection on the appropriate spectrum given the incident electron energy.

**S<sub>2</sub> Spectrum:** Intense band emission from the S<sub>2</sub> B  $^3\Sigma_u^- \leftarrow X^3\Sigma_u^-$  transition emits from 2800–6400Å [9].

Unfortunately there is a lack of laboratory spectra and cross sections for electron excitation of S<sub>2</sub>. We thus pre-compute the resultant spectra from each upper state vibrational level,  $\nu'$ , using the spectroscopic constants in [9] and the Frank-Condon factors obtained from Langhoff [10]. These spectra are then used to generate a photon wavelength for each excitation event, given  $\nu'$ . The probability for an excitation event to excite to a given  $\nu'$  is assumed to be proportional to the Franck-Condon factors. To determine the overall excitation rate to the B  $^3\Sigma_u^-$  state we use Garrett *et al.*'s [11] theoretical cross section versus electron energy. The resultant simulation spectrum is similar to that measured in a gas discharge [9].

**Surface Reflection:** Photoabsorption and scattering in Io's atmosphere can be neglected (maximum optical depth of ~0.1). However, it is important to account for the reflection of incident light off Io's frost-covered surface; the reflectivity of Io varies from ~0.05 to ~0.7 in the UV-V range [12] which affects the magnitude and shape of the spectrum. For each emission event, the spatially resolved reflected intensity is computed by "emitting" many (~10<sup>5</sup>) tracer photons towards Io with random orientations inside Io's solid angle as seen by the emitting particle. The number of tracer photons to hit a 1°×1° surface element is recorded and the contribution to the surface element brightness is computed assuming a Lambert surface.

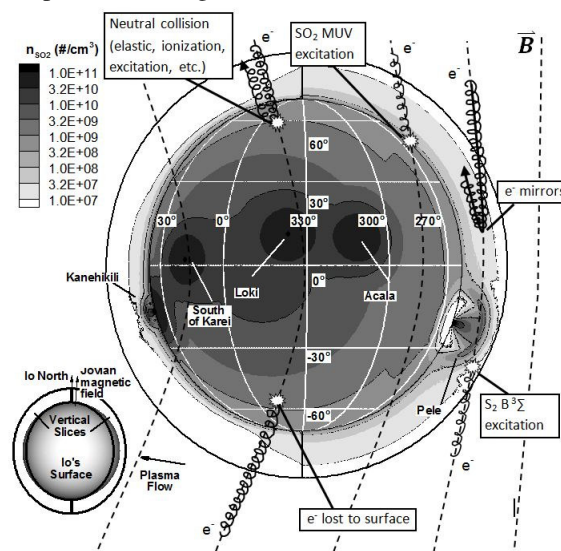


Figure 1: Electron transport model. The plasma flows from right to left and the electrons move along the dashed magnetic field lines and interact with the local neutral atmosphere (contours show the SO<sub>2</sub> density at the surface and in radial slices near each limb).

**Results:** Figure 2 shows the simulated line of sight cumulative emission from 2670–6000Å. Pele’s canopy above the limb and the surface below are very bright. Electron energy depletion across Surt causes the plume to be brighter in the north. Surt also “shields” Acala which is dimmer than the other visible small plumes (Masubi and Kanehikili). The small plumes are much dimmer than the Pele-type plumes because in our model they do not contain S<sub>2</sub> which has a much larger excitation cross section than SO<sub>2</sub> MUV2 excitation.

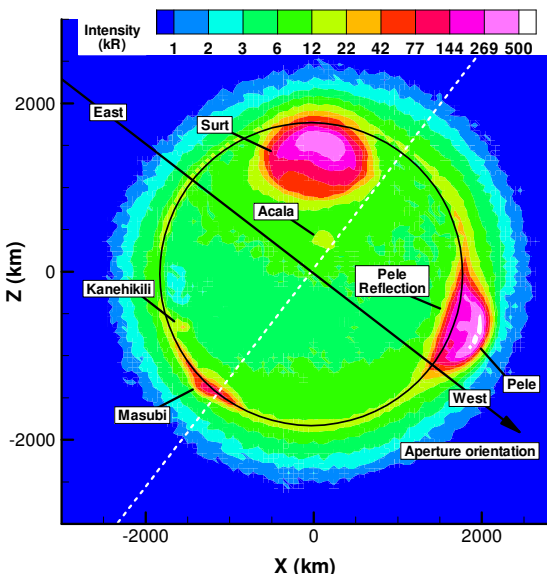


Figure 2: Simulated emission (from gas and reflected light).

By summing the spatially resolved spectra across Io into east and west halves (dashed white line), it might be possible to constrain volcanic activity. Specifically, Surt and Pele are very bright giant plumes (Figure 2) located in opposite halves of Io. In Figure 3 (left) the intensity for each half was independent of the other half’s volcanic activity. Figure 3 (right) shows that the activity of Pele-type plumes (including their S<sub>2</sub> content) dramatically effects the east/west intensity ratio, primarily above ~2800Å due to S<sub>2</sub> emission. When Pele and Surt are inactive, the east/west ratio is less than one due to the west’s larger SO<sub>2</sub> column. Comparison to the observation will be presented.

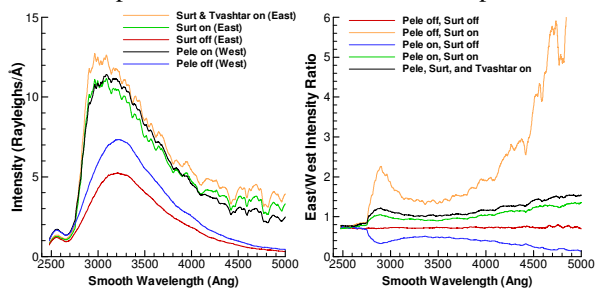


Figure 3: Left: East and West spectra for various plume activity levels. Right: Ratio of east/west spectra for each case.

The observed spectrum and several spectra simulated with assumed upstream thermal electron temperatures,  $T_e$ , of 4, 5, and 6eV are shown in Figure 4. Both the simulated and observed spectra are boxcar smoothed over 112Å. Above ~3400Å the solar spectrum refracted through Jupiter (not modeled) begins to dominate the observation.

The simulated peak intensity at ~3100Å for  $T_e=6\text{eV}$  agrees well with the observation, but the MUV1 peak intensity (~2550Å) does not unless the direct excitation of SO to the A <sup>3</sup>Π and B <sup>3</sup>Σ states (primary features of MUV1) is included. Since we have no data on the cross section for this excitation, we assume it is equal to the SO<sub>2</sub> MUV1 cross section with a shifted excitation threshold. Even with this conservative cross section, and an SO concentration of ~7% on the dayside, emission from direct excitation of SO dominates. Also, a non-thermal component of 30eV electrons (to be presented) should cause increased emission, bringing the  $T_e=5\text{eV}$  MUV2 peak inline with observations. Figure 4 also shows the intensity due to reflectance off the surface for the 5eV case. While the reflected intensity is relatively small, it does tend to level off the spectrum at longer wavelengths and is locally important.

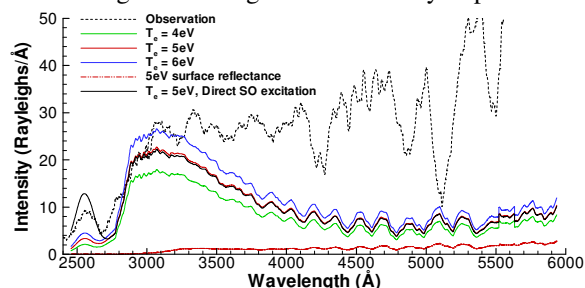


Figure 4: Spectra at several upstream electron temperatures.

**Conclusions:** Simulations of Io’s NUV-V emission spectrum in eclipse show that plumes, especially S<sub>2</sub>-rich Pele-type giant plumes, are bright. Their S<sub>2</sub> concentration and activity levels affect the absolute brightness as well as the east/west intensity ratio across Io which should allow for plume activity to be determined from observed NUV-V spectra. Direct excitation of SO seems to be important for modeling the MUV1 peak at 2550Å.

**Acknowledgements:** NASA Grant NNX08AQ49G

**References:** [1] Trafton et al. (2007) *MOP* 115. [2] Moore C.H. et al. (2006) *LPSC XXXVII*, Abstract #2281. [3] Moore C.H. et al. (2009) *Icarus*, In Press. [4] Combi, M.R., et al., *JGR* **103**, 9071-9081. [7] Geissler P. et al. (2004) *Icarus* **169**, 29-64. [8] Ajello J.M. et al. (2002) *JGR* **107**, A7, 2-1. [9] Peterson D.A. et al. (1980) *J. Chem. Phys.* **73**, 1551-1566. [10] Langhoff S.R., private communication. [11] Garrett B.C. et al. (1985) *Phys. Rev. A* **32**, 3366-3375. [12] Spencer J.R. et al. (2004) *Jupiter: The planet, satellites, and magnetosphere*. Cambridge Press, 689-698.